Journal of Biomechanics 207 (2026) 113555

Contents lists available at ScienceDirect

Journal of Biomechanics

journal homepage: www.elsevier.com/locate/jbiomech

Short communication

Effects of mechanical loading on cranial suture mesenchymal stem cell proliferation

Miranda Steacy [a,b,*], Ce Liang [a], Damith Suresh Chathuranga [a], Marius Didziokas [a], Tengyang Qiu [a,b], Dale Moulding [b], Ali Alazmani [c], Erwin Pauws [b,1], Mehran Moazen [a,1]

[a] Department of Mechanical Engineering, University College London, London, UK
[b] Developmental Biology and Cancer Research and Teaching Department, UCL Great Ormond Street Institute of Child Health, University College London, London, UK
[c] School of Mechanical Engineering, University of Leeds, Leeds, UK

ARTICLE INFO

Keywords:
Cyclic loading
Craniofacial system
Mechanobiology
Suture
Skull

ABSTRACT

Sutures are the primary sites of cranial bone growth, allowing the skull to accommodate the growing brain. External mechanical stimulus has been shown to delay suture fusion and induce tissue remodelling. Recent studies suggest that *in vivo* cyclic loading increased proliferation of mesenchymal stem cells (MSC) in the coronal suture. The overall aim of this study was to understand how many loading sessions (exposure–response) and how long after loading (time-course) did MSC proliferation increase in the coronal suture. In the exposure–response analysis, mice underwent 1, 3, or 5 loading sessions between Postnatal day 7 (P7) and P11, and in the time-course analysis, treated mice underwent 10 loading sessions between P7 and P21. Loading sessions were 10 min at a frequency of 1 Hz and a force of 10 g (0.1 N). The loading tip was positioned on the posterior aspect of the left frontal bone, dorsal to the coronal suture. EdU labels newly synthesised DNA during the S-phase of cell division, whereas PCNA is abundant in cells during the G1, S, G2, and M phases. The exposure–response analysis showed that when both markers are combined, proliferation levels can be interpreted after a minimum of five loading sessions, at which point a clear increase in proliferation is observed. In the time-course analysis, proliferation was highest immediately after the final treatment session. 24 h after the final loading session, the effects of mechanical loading gradually returned to baseline. The effect of mechanical loading on MSC proliferation is highly dependent on the number of loading sessions and the time point after treatment.

1. Introduction

The juvenile craniofacial skeleton is made of several bones joined together via mesenchymal stem cell-filled (MSC) fibrous joints, called sutures. Sutures are the primary sites of cranial bone growth, allowing the skull to accommodate the growing brain and enable skull flexibility during birth (Ang et al., 2022; Flaherty et al., 2016). In addition, sutures can receive and translate external mechanical stimuli directly affecting the overall shape of the skull, suture structure, and suture patency (Herring, 2008; Mao, 2002). Along with morphological changes to the craniofacial complex, an external mechanical stimulus can activate signalling pathways, up- or downregulate gene expression, and alter cellular behaviour (Kopher & Mao, 2003; Peptan et al., 2008; Wang & Mao, 2002).

Several *in vitro* studies have investigated the effects of external forces on craniofacial sutures, finding that tensile forces increase MSC proliferation, maintain suture patency, collagen fibre synthesis, and promote osteoblast differentiation (Ikegame et al., 2001; Tanaka et al., 2000; Tholpady et al., 2007; Yu et al., 2009). However, fewer studies have used *in vivo* models to study the mechanobiology of sutures, highlighting that external forces can delay suture fusion, induce craniofacial remodelling, and affect skull growth (Moazen et al., 2022; Peptan et al., 2008; Vij & Mao, 2006). For example, Kopher & Mao (2003) demonstrated that cyclic tensile mechanical loading of the rabbit nasofrontal suture maintained sutural patency and stimulated an anabolic sutural growth response. We recently showed that minimally invasive *in vivo* cyclic loading of the coronal suture (joining the frontal and parietal bones) in mice increased MSC proliferation (Steacy et al., 2026). This study's findings encouraged further investigation into the response time and exposure frequency needed to reach the observed cellular response.

* Corresponding author at: Department of Mechanical Engineering, University College London, London, UK.
E-mail address: miranda.steacy.22@ucl.ac.uk (M. Steacy).
[1] Contributed equally.

https://doi.org/10.1016/j.jbiomech.2026.113555
Accepted 31 August 2026
Available online 2 September 2026
0021-9290/© 2026 The Authors. Published by Elsevier Ltd. This is an open access article under the CC BY license (http://creativecommons.org/licenses/by/4.0/).

Two questions arose regarding the time to effect of this treatment on proliferation. The first is the number of cyclic loading sessions required to observe a change in cellular proliferation, an exposure–response analysis. The second is a time-course analysis to determine how long after a full round of treatment (10 loading sessions over 12 days) the cellular proliferation response persists.

The overall aim of this study was to understand how mechanical loading induces proliferation in the coronal suture. Specifically, we hypothesised that cyclic loading would gradually increase MSC proliferation with each additional treatment session, and that immediately after a full course of treatment, proliferation would increase, then decrease steadily over the following days.

2. Methods

2.1. Animals

A total of 35 CD-1 wild-type mice were used. In the exposure–response analysis, 18 animals were used, with 9 animals in each of the treated and untreated groups. In the time-course analysis, 17 animals were included; 8 underwent treatment, and 9 were used as controls. All the animals were used for histological analyses (n = 2 or 3 per group, 4 technical repeats).

Note: All animal experiments were approved by the UK Home Office and performed as part of a Project License (number: PP8161503) under the UK Animals (Scientific Procedures) Act 1986. Animal procedures complied with the ARRIVE guidelines and were performed under the supervision of UCL Biological Services.

2.2. Mechanical loading

The cyclical loading treatment was adapted from Moazen et al. (2022). An experimental loading set up was developed with an actuator (T-LSR series, Zaber Technologies: res. 50 μm, max. load 200 N) and a force sensor (GSO Series, Transducer Techniques: res. 0.01 N with 1 N capacity) configured to a custom developed LabVIEW program (National Instruments Corp, Austin, TX, USA), as illustrated in Fig. 1D.

In the exposure–response analysis, animals underwent 1, 3, or 5 loading sessions between postnatal (P) day 7 and P11 and were harvested at P7 (1 loading session), P9 (3 loading sessions), and P11 (5 loading sessions). In the time-course analysis, treated mice underwent 10 loading sessions between P7 and P18 and were harvested immediately after the 10th and final loading session (P18), or 24 h (P19) or 72 h (P21) later. Loading sessions were 10 min at a frequency of 1 Hz and a force of 10 g (0.1 N). Animals underwent one loading session once a day, administered between 9 am and 12 am. To maintain consistency, the order in which animals were treated each day remained the same. The 1 mm loading tip was placed on a drawn-on dot on the skin on the posterior aspect of the left frontal bone, anterior to the coronal suture, and lateral to the interfrontal suture (Fig. 1A).

2.3. EdU injections

Mice were intraperitoneally injected (50 mg/kg body weight) with 5-ethynyl-2′-deoxyuridine (EdU) (baseclick GmbH, Munich, Germany) 4 h prior to culling.

2.4. Histological analysis

Skulls were immediately fixed in 10% formalin at 4°C for 7 days. The

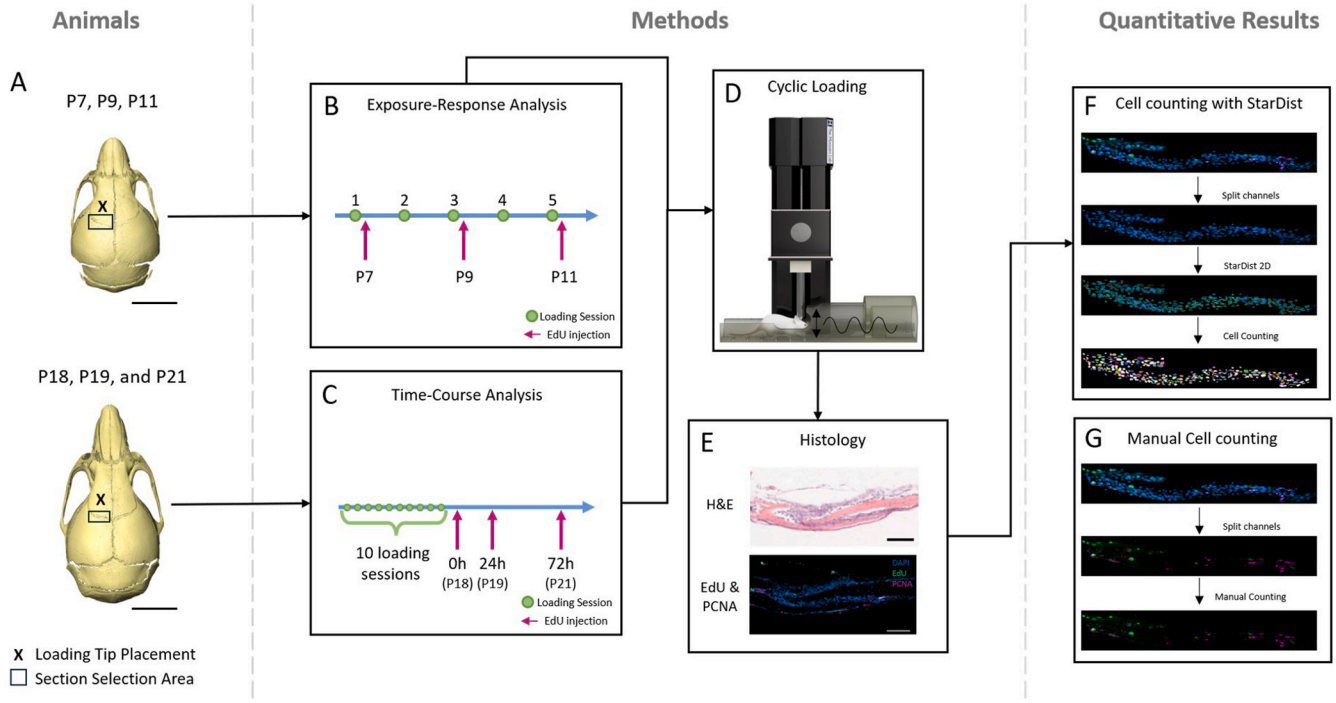


Fig. 1. An overview of the experimental workflow. (A) The animals in this experiment included P7, P9, and P11 mice as well as P18, P19, and P21 mice. The loading tip was placed on the posterior aspect of the left frontal bone, lateral to the interfrontal suture and anteriorly to the coronal suture. Histology sections included in the proliferation analysis were taken solely from the left coronal suture. (B) The first experiment undertaken was the exposure-response analysis. Mice underwent either one (P7), three (P9), or five (P11) loading sessions. Mice were injected with EdU right after their final loading session and collected 4 h after the IP injection. (C) The second experiment was a time-course analysis. Mice had 10 loading over the course of 12 days and were collected 0 h after loading (P18), 24 h after loading (P19), or 72 h after loading (P21). EdU was injected 4 h prior to collection. (D) Diagram of the mechanical cyclic loading experimental set up. (D) The histology done including H&E and IHC for proliferation markers EdU and PCNA. (F) DAPI stained cell counting of coronal suture cell in ImageJ with StarDist (with CSBDeep). (G) Manual counting of EdU and PCNA-stained cells.

fixed skulls were then washed in PBS and decalcified for 10 days in 20% EDTA at 4°C. The skulls were embedded in paraffin and sagittally sectioned 10 μm thick. Sections were stained with Haematoxylin and Eosin. Slides were imaged using the Zeiss Axioplan microscope.

2.5. Immunohistochemistry

Sagittal sections were then placed in sodium citrate (10 mM trisodium citrate, 0.5% Tween-20, pH) and underwent antigen retrieval in a steamer. EdU staining was done per the manufacture instructions. Proliferating Cell Nuclear Antigen (PCNA) (clone PC10(3F81), Invitrogen, 1:100) was diluted with PBST (0.01% Tween-20), 10% donkey serum, and 1% bovine serum albumin and applied overnight at 4°C. Secondary antibodies were applied with a 1:300 dilution. DAPI (4,6-diamidino-2-phylindole, Sigma) was pipetted and left for 10 min. Immunofluorescence imaging was done on the Zeiss Observer 7 at a 20x 1.0 NA.

2.6. Quantitative analysis

DAPI stained images were used to do cell counting in ImageJ (version 1.54i) (n = 2 or 3 per group, 4 technical replicates). An outline of the suture was manually drawn. Cell counting was done by StarDist 2D (with CSBDeep) with a Score Threshold of 0.5 and an overlap threshold of 0.4 (Fig. 1F) (Schmidt et al., 2018). EdU and PCNA-stained cells were manually counted (Fig. 1G) (n = 2 or 3 per group, 4 technical repeats).

2.7. Statistical analysis

For quantitative histological analyses, an unpaired *t*-test was selected because the study compared two independent experimental groups. Levene's test was used to assess the assumption of equal variances. Welch's correction was applied where appropriate to provide a more robust comparison when variances differed between groups. A significance threshold of $p < 0.05$ was used throughout.

3. Results

3.1. Exposure-response analysis

The exposure–response analysis investigated the number of cyclic loading sessions required to induce a change in proliferation. Mice underwent one, three, or five loading sessions. Immediately after the final loading session, they were injected with EdU and culled 4 h later.

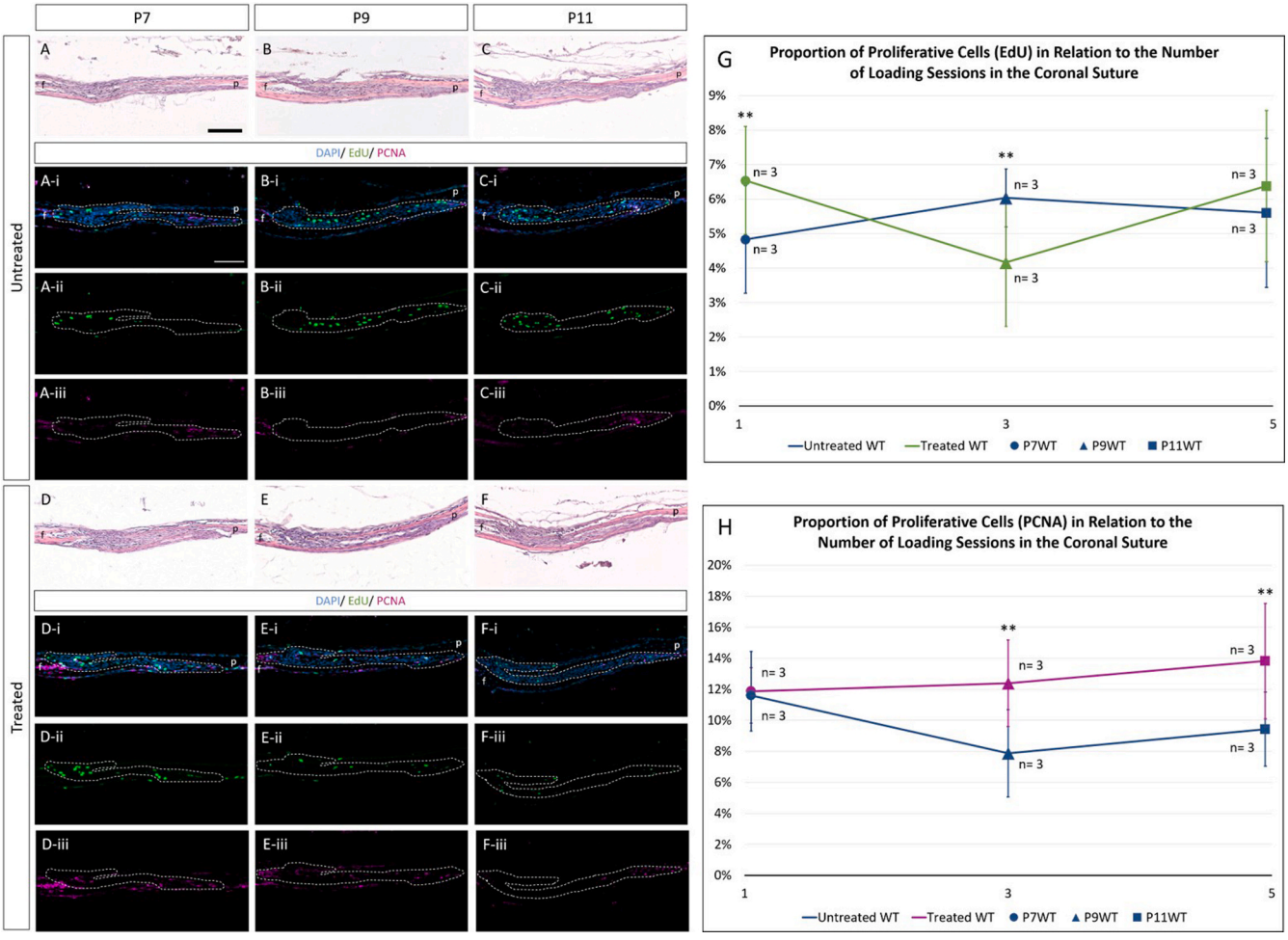


Fig. 2. Exposure-response analysis at P7 (one loading session), P9 (three loading sessions), and P11 (five loading sessions). (A-C, D-F) H&E-stained sagittal sections for the coronal suture in treated (loaded) and control (unloaded) animals. (i) Immunohistochemistry composites of sagittal sections for the coronal suture stained for DAPI (blue), EdU (green), and PCNA (magenta). Dashed line outlining the coronal suture. (ii) Single channel immunohistochemistry of EdU. (iii) Single channel immunohistochemistry of PCNA. f: frontal, p: parietal. Scale bar: 100 μm. (G) Exposure-response graph showing the proportion of proliferative cells (EdU) in the coronal suture cells after one, three, and five loading sessions. (H) Exposure-response graph showing the proportion of proliferative cells (PCNA) in the coronal suture cells after one, three, and five loading sessions. (n = 3, 4 technical replicates per group) (** $p < 0.01$). (For interpretation of the references to colour in this figure legend, the reader is referred to the web version of this article.)

Consequently, mice receiving one loading session were culled at P7, whereas those receiving three and five loading sessions were culled at P9 and P11, respectively. After one loading session, within the coronal suture, P7-treated animals had a proportion of proliferative EdU-stained cells of 6.54% (s.d. 1.56%) and PCNA-stained cells of 11.87% (s.d. 1.79%) (Fig. 2). Their time-matched control animals had proliferation proportions of 4.83% (1.48%) and 11.60% (s.d. 2.57%) for EdU and PCNA, respectively. The increase in proliferation at P7 after one loading treatment was statistically significant for the EdU proportion ($p < 0.01$) but not for the PCNA proportion. At P9, after 3 loading sessions, the proportion of EdU-stained cells in the treated animals was 4.16% (s.d. 1.85%) and PCNA-stained cells was 12.39% (s.d. 2.79%). In the control P9 mice, the proportion of EdU-positive cells in the coronal suture was 6.03% (s.d. 0.84%) and 7.87% (s.d. 2.82%) for PCNA-positive cells. The PCNA-staining at this time point shows a statistically significant increase in proliferation after 3 loading sessions ($p < 0.001$). In contrast, the EdU-staining shows a statistically significant decrease in proliferation after 3 loading sessions ($p < 0.008$). Finally, at P11 and after 5 loading sessions, treated animals had proliferation proportions of 6.38% (s.d. 0.84%) and 13.82% (s.d. 3.72%) for EdU and PCNA, respectively. The control P11 animals had proliferation proportions of 5.60% (s.d. 2.16%) and 9.43% (s.d. 2.39%). The increase in PCNA-positive cells in the treated animals was statistically significant after five loading sessions ($p < 0.002$).

3.2. Time-course analysis

After two weeks of cyclic loading, mice were collected immediately after treatment (0 h, P18), one day after treatment (24 h, P19), or three days after treatment (72 h, P21) (Fig. 3). P18-treated mice had an average EdU proliferation percentage of 3.41% (s.d. 2.18%), whereas their age-matched controls had 1.24% (s.d. 0.89%) EdU-positive cells in the coronal suture. The P18-treated animals had an average of 22.17% (s.d. 3.87%) positive PCNA-stained cells. The age-matched controls had a proportion of PCNA-positive cells of 15.51% (s.d. 5.32%). At P18, the increase in EdU and PCNA-positive cells in the treatment group was statistically significant ($p < 0.02$ and $p < 0.008$, respectively). In the P19 mice, treated animals had an EdU-positive cell percentage of 2.93% (s.d. 2.17%) and a PCNA-positive cell percentage of 23.85% (s.d. 6.22%). P19 untreated mice had an EdU staining percentage of 2.11% (s.d. 1.13%) and a PCNA staining percentage of 16.57% (s.d. 4.69%). In P19 mice culled 24 h after the last loading session, the increase in proliferation was statistically significant for the PCNA marker ($p < 0.01$), whereas the increase in EdU-positive cells was not statistically significant. Mice that were culled 72 h after treatment at P21 had an EdU proliferation

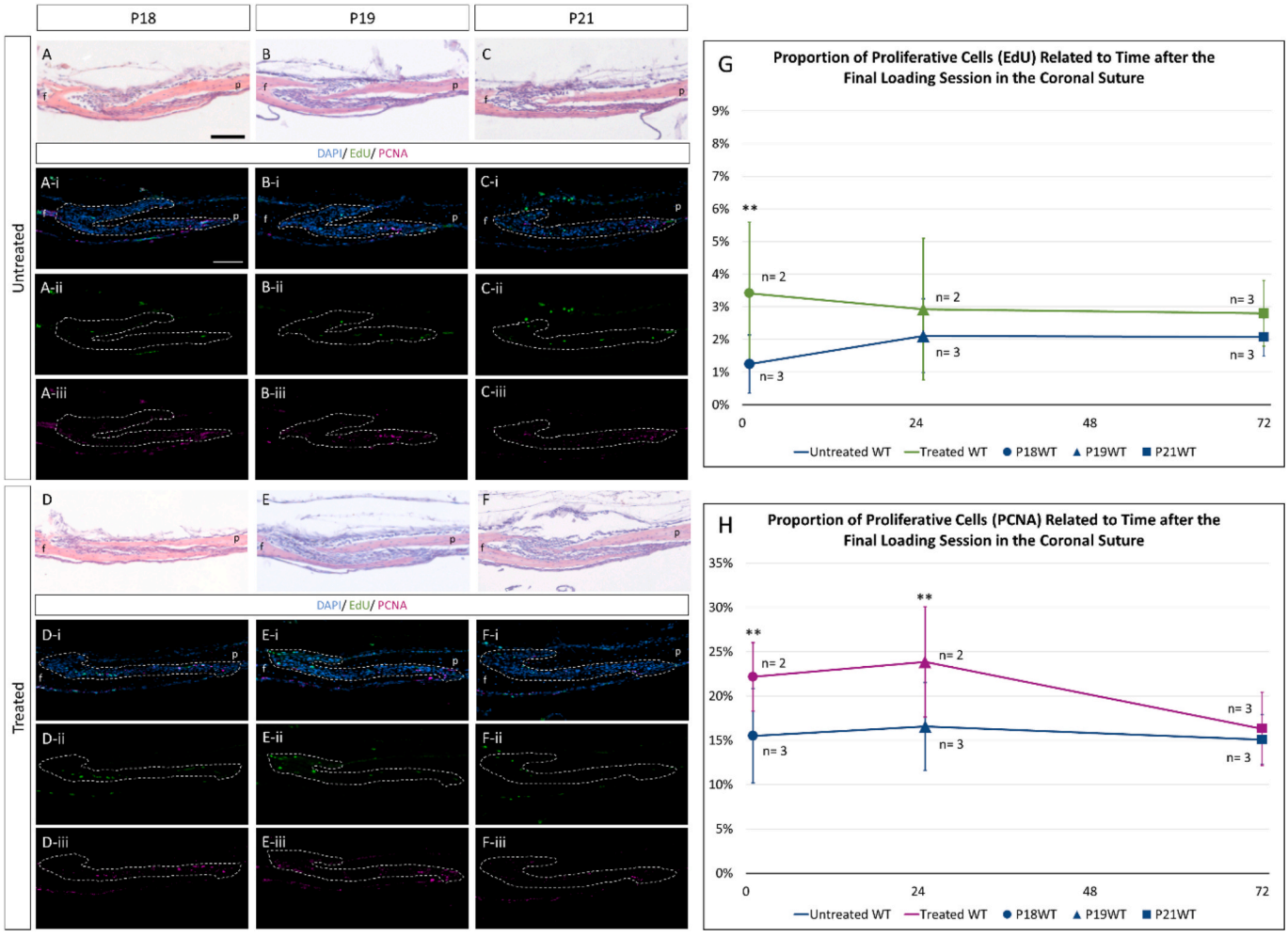


Fig. 3. Time-course analysis at P18 (0 h after 10 loading sessions), P19 (24 h after 10 loading sessions), and P21 (72 h after 10 loading sessions). (A-C, C-F) H&E-stained sagittal sections for the coronal suture in treated (loaded) and control (unloaded) animals. (i) Immunohistochemistry composites of sagittal sections for the coronal suture stained for DAPI (blue), EdU (green), and PCNA (magenta). Dashed line outlining the coronal suture. (ii) Single channel immunohistochemistry of EdU. (iii) Single channel immunohistochemistry of PCNA. f: frontal, p: parietal. Scale bar: 100 μm. (G) Time-course graph showing the proportion of proliferative cells (EdU) in the coronal suture cells 0 h, 24 h, and 72 h after 10 loading sessions. (H) Time-course graph showing the proportion of proliferative cells (PCNA) in the coronal suture cells 0 h, 24 h, and 72 h after 10 loading sessions. ($n = 2$ or 3, 4 technical replicates per group) (** $p < 0.01$). (For interpretation of the references to colour in this figure legend, the reader is referred to the web version of this article.)

percentage of 2.80% (s.d. 1.01%), and in untreated animals, 1.84% (s.d. 0.58%). The P21-treated animals had a PCNA-positive percentage of 16.30% (s.d. 4.13%), and untreated animals had a PCNA-positive percentage of 15.10% (s.d. 2.82%). Proliferation was not statistically significant at P21, 72 h after treatment (Table 1).

4. Discussion

Our recent study found that cyclic loading of coronal suture increases MSC proliferation in the coronal suture (Steacy et al., 2026). This study aimed to further investigate the exposure frequency and response time needed to reach peak MSC proliferation. The main finding of the exposure–response analysis was that cyclic loading increased EdU-positive cells after one loading sessions and decreased after three loading sessions, whereas PCNA-positive cells increased after three and five loading sessions. In the time-course analysis, the main finding from both the EdU and PCNA markers was that immediately after the final treatment session, proliferation peaked, and 24 h after the final loading session, the effects of cyclic mechanical loading gradually returned to baseline.

EdU labels newly synthesised DNA during the S-phase of cell division, whereas PCNA is abundant in cells during the G1, S, G2, and M phases (Mead & Lefebvre, 2014). The combined use of EdU and PCNA allows for a broader assessment of the cellular response to cyclic loading to answer whether cyclic loading induces new DNA synthesis immediately following treatment or whether the treatment increases the proportion of cells entering the proliferative cycle. The higher percentage of PCNA-positive cells seen in the coronal suture can be explained by its presence throughout a greater proportion of the cell cycle, its persistence half-life of around 20 h, meaning it remains in the cell for 24 to 48 h in newly quiescent cell. Additionally, PCNA accumulates at sites of DNA damage without a corresponding increase in EdU (Chapman & Wolgemuth, 1994; Essers et al., 2005; McCarty, 2007).

The main discrepancy between the EdU and PCNA markers in this study lies in the exposure–response analysis. After 3 loading sessions, EdU shows a decrease in proliferation, whereas PCNA shows an increase. The EdU result was inconsistent with the initial hypothesis that cyclic loading would gradually increase MSC proliferation with each additional treatment session. Both markers are widely used and considered highly reliable (Mead & Lefebvre, 2014). Therefore, neither proliferation marker can be discounted solely on the results from this study. One explanation for this difference could be the limited number of animals included in this study. Kulldorff et al., (2000) found that the correlations between BrdU and PCNA assays vary substantially based on the number of biopsies obtained for each individual, emphasising the importance of having a large number of participants in cell proliferation measurement studies. Altogether, the exposure–response analysis showed that when the results of both markers are combined, levels of proliferation cannot be interpreted until at least five loading sessions have been completed, at which point a significant increase in PCNA and a non-significant increase in EdU proliferation is observed. Tholpady et al., (2007), found similar results, when sutures were artificially maintained open by tensile force the increase in proliferative cells was not apparent as early as 1 week but was very clear in the second week.

PCNA showed that loading had a cumulative effect on proliferation. Proliferation was 11.87%, 12.39%, and 13.82% after one, three, and five loading sessions, respectively. Kaspar et al., (2002) found that in human bone-derived osteoblast-like cells, proliferation increases with the number of applied cycles until a maximum cycle number is reached. Exposure-response analyses tend to emphasise the 'therapeutic window', highlighting the cumulative, plateauing then adverse effects of external loading. Guo, (2026) illustrates this with a step-line showing the gradual increase in proliferation, over a 3 to 14 day window, followed by a plateau. In this study, the treatment remained in the 'therapeutic window' and the time-course analysis corroborated the sustained positive effects of the treatment protocol.

The time-course analysis, where proliferation was sustained for 24 h after the last treatment session, aligns with the hypothesis and other studies investigating the onset and duration of proliferation after loading. In explant culture and *in vivo*, cell proliferation increases upon tensile strain for 24 h and declines 72 h post-treatment (Hickory & Nanda, 1987; Mizukoshi et al., 2021).

The main limitation of this study was the number of animals included. Due to the labour-intensive nature of the cyclic loading, only nine animals could be treated in one day. In the future, it would be important to repeat this protocol on more animals to increase the n-numbers, which may shed light on the EdU and PCNA marker discrepancies observed in the exposure–response analysis.

5. Conclusion

The exposure–response analysis demonstrates that cellular responses to cyclic loading are cumulative, with a minimum of five treatment sessions at 1 Hz and a force of 10 g (0.1 N) required to see a measurable increase in proliferation. The time-course analysis indicates that these molecular effects diminish once treatment ends, highlighting the importance of carefully considering the timing of tissue collection in future studies. The findings of this study contribute to the growing body of research investigating the biological effects of cyclic loading with the hope of future clinical translation.

Declaration

All authors contributed to the study's conception and design. Specimen preparation was performed by Miranda Steacy, Ce Liang, Damith Suresh Chathuranga, Marius Didziokas, Tengyang Qiu, and Erwin Pauws. The custom loading set up was developed by Ali Alazmani. All histology and image processing was performed by Miranda Steacy with the guidance of Dale Moulding. All statistical analysis was done by Miranda Steacy. The first draft of the manuscript was written by Miranda Steacy. All authors commented on previous versions of the manuscript. All authors read and approved the final manuscript. Mehran Moazen and Erwin Pauws supervised the project and secured the funding.

CRediT authorship contribution statement

Miranda Steacy: Writing – original draft, Methodology, Investigation, Formal analysis, Data curation, Conceptualization. **Ce Liang:**

Table 1
Summary of EdU and PCNA proliferation proportions for the exposure–response and time-course analysis.

Exposure-response analysis				Time-course analysis			
		EdU	PCNA			EdU	PCNA
P7	Untreated	4.83%	11.60%	P18	Untreated	1.24%	15.51%
(1 session)	Treated	6.54%	11.87%	(0 h)	Treated	3.41%	22.17%
P9	Untreated	6.03%	7.87%	P19	Untreated	2.11%	16.57%
(3 sessions)	Treated	4.16%	12.39%	(24 h)	Treated	2.93%	23.85%
P11	Untreated	5.60%	9.43%	P21	Untreated	1.84%	15.10%
(5 sessions)	Treated	6.38%	13.82%	(72 h)	Treated	2.80%	16.30%

Writing – review & editing, Data curation. **Damith Suresh Chathuranga:** Writing – review & editing, Data curation. **Marius Didziokas:** Writing – review & editing, Data curation. **Tengyang Qiu:** Writing – review & editing, Data curation. **Dale Moulding:** Writing – review & editing, Methodology. **Ali Alazmani:** Writing – review & editing, Software. **Erwin Pauws:** Writing – review & editing, Supervision, Resources, Project administration. **Mehran Moazen:** Writing – review & editing, Supervision, Resources, Project administration, Funding acquisition, Conceptualization.

Funding

This work was supported by the Engineering and Physical Science Research Council (EP/W008092/1; EP/R513143/1-2592407 and EP/T517793/1-2592407) and the NIHR Great Ormond Street Hospital Biomedical Research Centre, United Kingdom.

Declaration of competing interest

The authors declare the following financial interests/personal relationships which may be considered as potential competing interests: Mehran Moazen and Erwin Pauws reports financial support was provided by Engineering and Physical Sciences Research Council. Mehran Moazen and Erwin Pauws reports financial support was provided by NIHR Great Ormond Street Hospital Biomedical Research Centre. If there are other authors, they declare that they have no known competing financial interests or personal relationships that could have appeared to influence the work reported in this paper.

References

Ang, P.S., Matrongolo, M.J., Zietowski, M.L., Nathan, S.L., Reid, R.R., Tischfield, M.A., 2022. Cranium growth, patterning and homeostasis. Development 149 (22). https://doi.org/10.1242/dev.201017.

Chapman, D.L., Wolgemuth, D.J., 1994. Expression of proliferating cell nuclear antigen in the mouse germ line and surrounding somatic cells suggests both proliferation-dependent and -independent modes of function. Int. J. Dev. Biol. 38 (3), 491–497.

Essers, J., Theil, A.F., Baldeyron, C., van Cappellen, W.A., Houtsmuller, A.B., Kanaar, R., Vermeulen, W., 2005. Nuclear dynamics of PCNA in DNA replication and repair. Mol. Cell. Biol. 25 (21), 9350–9359. https://doi.org/10.1128/mcb.25.21.9350-9359.2005.

Flaherty, K., Singh, N., Richtsmeier, J.T., 2016. Understanding craniosynostosis as a growth disorder. Wiley Interdiscip. Rev. Dev. Biol. 5 (4), 429–459. https://doi.org/10.1002/wdev.227.

Guo, D., 2026. The regulatory effects of mechanical loading on cellular behavior during tendon-bone healing. Mater. Des. 261, 115364. https://doi.org/10.1016/j.matdes.2025.115364.

Herring, S.W., 2008. Mechanical influences on suture development and patency. Front. Oral Biol. 12, 41–56. https://doi.org/10.1159/0000115031.

Hickory, W.B., Nanda, R., 1987. Effect of tensile force magnitude on release of cranial suture cells into S phase. Am. J. Orthod. Dentofac. Orthop. 91 (4), 328–334. https://doi.org/10.1016/0889-5406(87)90175-2.

Ikegame, M., Ishibashi, O., Yoshizawa, T., Shimomura, J., Komori, T., Ozawa, H., Kawashima, H., 2001. Tensile stress induces bone morphogenetic protein 4 in preosteoblastic and fibroblastic cells, which later differentiate into osteoblasts leading to osteogenesis in the mouse calvariae in organ culture. J. Bone Miner. Res. 16 (1), 24–32. https://doi.org/10.1359/jbmr.2001.16.1.24.

Kaspar, D., Seidl, W., Neidlinger-Wilke, C., Beck, A., Claes, L., Ignatius, A., 2002. Proliferation of human-derived osteoblast-like cells depends on the cycle number and frequency of uniaxial strain. J. Biomech. 35 (7), 873–880. https://doi.org/10.1016/S0021-9290(02)00058-1.

Kopher, R.A., Mao, J.J., 2003. Suture growth modulated by the oscillatory component of micromechanical strain. J. Bone Miner. Res. 18 (3), 521–528. https://doi.org/10.1359/jbmr.2003.18.3.521.

Kulldorff, M., McShane, L.M., Schatzkin, A., Freedman, L.S., Wargovich, M.J., Woods, C., Purewal, M., Burt, R.W., Lawson, M., Mateski, D.J., Lanza, E., Corle, D.K., O'Brien, B., Moler, J., 2000. Measuring cell proliferation in the rectal mucosa: comparing bromodeoxyuridine (BrdU) and proliferating cell nuclear antigen (PCNA) assays. J. Clin. Epidemiol. 53 (8), 875–883. https://doi.org/10.1016/S0895-4356(99)00180-8.

Mao, J.J., 2002. Mechanobiology of craniofacial sutures. J. Dent. Res. 81 (12), 810–816. https://doi.org/10.1177/154405910208101203.

McCarty, G. A., 2007. Proliferating cell nuclear antigen autoantibodies. In *Autoantibodies* (pp. 205–210). Elsevier. https://doi.org/10.1016/B978-044452763-9/50031-7.

Mead, T.J., Lefebvre, V., 2014. Proliferation Assays (BrdU and EdU) on Skeletal Tissue Sections. In: Hilton, M. (Ed.), Skeletal Development and Repair. Methods in Molecular Biology, vol. 1130. Humana Press, Totowa, NJ, pp. 233–243. https://doi.org/10.1007/978-1-62703-989-5_17.

Mizukoshi, M., Kaku, M., Thant, L., Kitami, K., Arai, M., Saito, I., Uoshima, K., 2021. In vivo cell proliferation analysis and cell-tracing reveal the global cellular dynamics of periodontal ligament cells under mechanical-loading. Sci. Rep. 11 (1). https://doi.org/10.1038/s41598-021-89156-w.

Moazen, M., Hejazi, M., Savery, D., Jones, D., Marghoub, A., Alazmani, A., Pauws, E., 2022. Mechanical loading of cranial joints minimizes the craniofacial phenotype in Crouzon syndrome. Sci. Rep. 12 (9693), 1–11. https://doi.org/10.1038/s41598-022-13807-9.

Peptan, A.I., Lopez, A., Kopher, R.A., Mao, J.J., 2008. Responses of intramembranous bone and sutures upon in vivo cyclic tensile and compressive loading. Bone 42 (2), 432–438. https://doi.org/10.1016/j.bone.2007.05.014.

Schmidt, U., Weigert, M., Broaddus, C., Myers, G., 2018. *Medical image computing and computer assisted intervention – MICCAI 2018* (A. F. Frangi, J. A. Schnabel, C. Davatzikos, C. Alberola-López, & G. Fichtinger, Eds.; Vol. 11071). Springer International Publishing. https://doi.org/10.1007/978-3-030-00934-2.

Steacy, M., Didziokas, M., Qiu, T., Chathuranga, D.S., Liang, C., Alazmani, A., Moulding, D., Gardner, O., Moazen, M., Pauws, E., 2026. Mechanical bone loading effects on morphology and mechanobiology in the coronal suture of Crouzon mice. Open Biol. 16 (4). https://doi.org/10.1098/rsob.250387.

Tanaka, E., Miyawaki, Y., Tanaka, M., Watanabe, M., Lee, K., del Pozo, R., Tanne, K., 2000. Effects of tensile forces on the expression of type III collagen in rat interparietal suture. Arch. Oral Biol. 45 (12), 1049–1057. https://doi.org/10.1016/S0003-9969(00)00083-2.

Tholpady, S.S., Freyman, T.F., Chachra, D., Ogle, R.C., 2007. Tensional forces influence gene expression and sutural state of rat calvariae in vitro. Plast. Reconstr. Surg. 120 (3), 601–611. https://doi.org/10.1097/01.prs.0000270284.69632.6b.

Vij, K., Mao, J.J., 2006. Geometry and cell density of rat craniofacial sutures during early postnatal development and upon in vivo cyclic loading. Bone 38 (5), 722–730. https://doi.org/10.1016/j.bone.2005.10.028.

Wang, X., Mao, J.J., 2002. Chondrocyte proliferation of the cranial base cartilage upon in vivo mechanical stresses. J. Dent. Res. 81 (10), 701–705. https://doi.org/10.1177/154405910208101009.

Yu, J.C., Chen, J.-R., Lin, C.-H., Zhang, G., Lam, P.-S., Wenger, K.H., Mozaffari, F.B., Huang, S.-T., Borke, J.L., 2009. Tensile strain-induced Ets-2 phosphorylation by CaMKII and the homeostasis of cranial sutures. Plast. Reconstr. Surg. 123 (Supplement), 83S–93S. https://doi.org/10.1097/PRS.0b013e318191c029.